



Indian Journal of Experimental Biology  
Vol. 58, September 2020, pp. 617-630



## Protective role of antioxidative enzymes and antioxidants against iron-induced oxidative stress in the cyanobacterium *Anabaena sphaerica* isolated from iron rich paddy field of Chhattisgarh, India

Kikku Kunui<sup>1</sup> & Satya Shila Singh<sup>2\*</sup>

<sup>1</sup>Department of Botany, Guru Ghasidas Vishwavidyalaya, Bilaspur-495 009, Chhattisgarh, India

<sup>2</sup>Department of Botany, Banaras Hindu University, Varanasi-221 005, Uttar Pradesh, India

Received 23 January 2018; revised 24 August 2019

Iron, as an essential element for plants and microorganisms, plays a significant role in photosynthesis, photopigment synthesis, nitrogen fixation, nucleic acid synthesis, etc. However, in iron rich environments, it causes stress by affecting various physiological activities including ROS generation and detoxification machineries. Here, we investigated the protective role of antioxidative enzymes and antioxidants against iron-induced oxidative stress in the cyanobacteria, *Anabaena sphaerica* from the iron rich regions of Chhattisgarh. We evaluated various morpho-physiological modifications at different concentrations of iron (0, 20, 50, 75 and 100  $\mu\text{M}$   $\text{FeCl}_3$ ). Microscopic and physiological characterization showed highest order of structural deformities, reactive oxygen species (ROS) generation and lipid peroxidation at 100  $\mu\text{M}$   $\text{FeCl}_3$  but growth was reduced only by 28%. Possibly, maximum superoxide dismutase (SOD) and ascorbate peroxidase (APX) activities along with highest level of antioxidants (carotenoid, proline, cysteine and non protein thiol) played a major role in protecting the growth. As compared to 20  $\mu\text{M}$   $\text{FeCl}_3$  treated cells of *A. sphaerica*, almost equal growth and no structural alterations at 50 and 75  $\mu\text{M}$   $\text{FeCl}_3$  may be correlated with minimum ROS, electrolyte leakage and malondialdehyde (MDA) content along with an activation of efficient ROS detoxification machinery i.e. enhanced level of antioxidative enzymes and antioxidants. Thus, the inherited property of *A. sphaerica* to grow at iron enriched condition make it more efficient microbe for improvement of the nitrogen status in the soil.

**Keywords:** Abiotic stress, Ascorbate peroxidase, Bioremediation, Cysteine, Heavy metal, Iron tolerance, Non protein thiol, Proline, Reactive oxygen species (ROS)

Iron is a limiting nutrient found on the earth's crust and plays a significant role in photosynthesis, photopigment synthesis, nitrogen fixation, nitrogen assimilation and nucleic acid synthesis, etc<sup>1</sup>. It also plays an important role in formation of structural skeleton of nitrogenase enzyme in form of Fe-Mo protein<sup>1</sup>. In spite of its importance in crucial life supporting activities, its availability to the plants and microorganisms is limited. Iron generally posses 2 oxidation state ferrous Fe (II) and ferric Fe (III). Fe (III) form of iron is thermodynamically stable and bears less soluble nature<sup>2</sup>. The ferric form of iron is generally found in oxygenic environment due to alkaline pH resulting in the formation of unavailable form of iron (ferric oxides and ferric hydroxides). However, plants and microorganisms synthesize siderophores that converts the unavailable form of iron

into the available form (ferrous) which is transported into the cell to fulfil their cellular iron requirements<sup>2</sup>.

Chhattisgarh, situated at one of the hot torrid zones of India, is known for its tropical climatic condition and edaphic factors which makes the soil suitable for paddy cultivation and also rich cyanobacterial diversity. Considering the importance of iron for plants and microorganisms and the luxuriant growth of cyanobacteria in the iron rich regions of Chhattisgarh, we investigated the effect of iron on the structural and functional organization of cyanobacteria. Though studies on the effects of iron on various physiological activities including ROS generating system and ROS detoxifying machinery of different cyanobacteria are common<sup>2-4</sup>, literature is silent on isolation and characterization of cyanobacterium from iron rich regions. Hence, we have made an attempt to investigate the defence strategies against iron-induced oxidative stress in the cyanobacterium *Anabaena sphaerica* isolated from the iron rich paddy fields of Chhattisgarh.

\*Correspondence:

Phone: +91 7587231571 (Mob.)

E-mail: [satyashila@rediffmail.com](mailto:satyashila@rediffmail.com)

## Materials and Methods

### Chemicals and reagents

Methanol, sodium hydroxide, Phenol, concentrated Sulphuric acid, Folin ciocalteau solution, Trichloroacetic acid (TCA), Potassium iodide,  $\beta$ -mercaptoethanol, Triton-X 100, Sodium ascorbate, Nitroblue tetrazolium (NBT), Ethylene diamine tetra acetic acid (EDTA), Riboflavin, Hydrogen Peroxide, Ascorbic acid, Sulphosalicylic acid, Ninhydrin, Glacial acetic acid, Orthophosphoric acid, Perchloric acid, DTNB [5'5'-dithio-bis - (2-nitrobenzoic acid)] were purchased from Hi Media laboratories (Mumbai, India). DCFH-DA (2'7' dichlorofluorescein-diacetate) for Reactive oxygen species determination within the cell was purchased from Sigma- Aldrich (St. Louis, USA). All the chemicals and reagents used for experiments were of analytical grade.

### Sampling sites

A number of cyanobacterial species were isolated from different paddy fields of Chhattisgarh, India enriched with iron content and the soil samples were analyzed to measure the iron content using atomic absorption spectrophotometer (AAS). The maximum iron concentration was found to be in the soil of Turkadih, Bilaspur, Chhattisgarh (140 ppm).

### Maintenance of culture

*Anabaena sphaerica* (NCBI-634399051; 16S rRNA accession number KJ774521), was isolated, identified and characterized from the soil of Turkadih, Bilaspur, Chhattisgarh, India on the basis of standard literature<sup>5,6</sup>. The axenic culture was maintained in BG-11 nutrient medium (pH 7.2) at standard growth condition<sup>5,7</sup>.

### Experimental design

Before experimentations, the axenic cultures of the cyanobacterium *Anabaena sphaerica* were transferred into iron deprived BG-11 medium for 8 days at the standard growth condition in the culture room. Then after, different concentrations of iron ( $\text{FeCl}_3$ ) were used i.e. 0, 20, 50, 75, 100, 125 and 150  $\mu\text{M}$  to observe different morphophysiological characters under iron stress. Growth was observed for 10 days under different iron stress condition whereas rest of the parameters i.e. SEM and confocal microscopic analysis, antioxidative enzymes, antioxidants, ROS generation, electrolyte leakage, MDA content and cellular  $\text{H}_2\text{O}_2$  content were investigated after 4 days of incubation.

### Direct absorbance and specific growth rate (k)

Exponentially grown cyanobacterial cultures were inoculated in sterilized Erlenmeyer flask containing

different concentration of iron (0, 20, 50, 75 & 100  $\mu\text{M}$ ) for 10 days at standard growth condition in culture room. Growth of *Anabaena sphaerica* was measured by taking optical density ( $\text{O.D}_{663}$ ) of the cultures withdrawn from the above flasks at every alternate day with the help of UV-Vis Spectrophotometer (Elico SL 210). The specific growth rate (k) was calculated using formula given by Kratz and Myers<sup>8</sup>.

### Determination of chlorophyll a, carotenoid and phycobillin content

About 5 mL of culture was centrifuged at 8000  $\times g$  for 5 min. The obtained pellet was left for 1.0 h with 3 mL methanol. The methanol extracted culture was re-centrifuged at 8000  $\times g$  for 5 min and supernatant was taken for estimation of chlorophyll-a and carotenoid. The supernatant of methanol extracted culture was taken for estimation of chlorophyll-a and carotenoid<sup>9</sup>. The left pellet after chlorophyll estimation was suspended in 5 mL potassium phosphate buffer (pH 6.8) for overnight. The suspended culture was centrifuged at 8000  $\times g$  for 5 min and pellet obtained was re-extracted with 5 mL potassium phosphate buffer (pH 6.8) for 3-4 times. The pellet was suspended in phosphate buffer (pH 6.8) for determination of total phycobillin content (sum of total allophycocyanin, phycocyanin and phycoerythrin)<sup>10,11</sup>.

### Estimation of protein and carbohydrate

The protein content was determined using Lysozyme as a standard<sup>12</sup>. Five mL of NaOH was added in the 0.5 mL of clear suspension culture and boiled for 10 min in water bath (60°C) and further 2.5 mL of freshly prepared solution of sodium carbonate and copper sulphate with sodium potassium tartarate was added. After mixing properly, 0.5 mL Folin ciocalteau solution (1 N) was added. Blue coloured solution was obtained and absorbance was taken at 650 nm.

To determine the carbohydrate content, 1.0 mL clear suspension culture was taken and treated with 1 mL phenol (5 % w/v). After mixing properly, 5 mL conc.  $\text{H}_2\text{SO}_4$  was added and kept for 10 min in water bath (30°C). The absorbance of yellow colour solution was taken at 485 nm<sup>13</sup>.

### Morphological attributes, Heterocyst frequency and Nitrogenase activity

The shape and size of vegetative cells and heterocysts of *A. sphaerica* were described on the basis of light, confocal and scanning electron microscopy (SEM). The heterocyst frequency was

determined as per the protocol of Singh *et al.*<sup>14</sup> whereas nitrogenase activity was estimated as per the protocol of Mishra & Singh<sup>15</sup>. The nitrogenase activity was determined as reported by others and expressed in terms of C<sub>2</sub>H<sub>4</sub> produced/mg protein/h.

#### **Determination of reactive oxygen species, cellular H<sub>2</sub>O<sub>2</sub>, MDA content and Electrolyte leakage**

Intracellular ROS formation was determined with the help of fluorescent probe DCFH-DA (dichlorodihydro-fluoresceindiacetate) that binds with the ROS in the absence of light. The samples were observed under Dewinter-fluorescence microscope.

Four day old cultures (1.0 mL) were taken from different concentrations of iron and were crushed with 0.1% trichloroacetic acid (TCA) (1.0 mL) for estimation of cellular H<sub>2</sub>O<sub>2</sub> content<sup>16</sup>. Then centrifugation was done at 8000 ×g for 10 min. The obtained supernatants were mixed with 1.0 mL 50 mM potassium-phosphate buffer (pH 7.0) and 1.5 mL potassium iodide (1 M). The absorbance of the sample was taken at 390 nm.

To determine the MDA content in the cell, 2 mL of 0.1% TCA was added to 1.0 mL homogenized cultures and left for 10 min. Further, 4 mL of 0.5% 2-thiobarbituric acid (TBA) prepared in 20% TCA solution was added and incubated in water bath (95°C, 30 min) and cooled immediately in ice bath to terminate the reaction. The above prepared samples were centrifuged at 10000 ×g for 10 min. The absorbance value of the supernatant taken at 532 and 600 nm were subtracted and MDA content was calculated with the help of 155 /mM/cm extinction coefficient<sup>3,14,17</sup>.

The cyanobacterium treated with different concentrations of iron was placed in the water bath for 32°C for 2 h and the initial electrical conductivity was measured as EC<sub>1</sub>. After measurement of EC<sub>1</sub>, the same samples were allowed to autoclave at 121°C for 20 min and cooled at room temperature (26°C). The final electrical conductivity was measured as EC<sub>2</sub>. The electrolyte leakage was measured using the formula  $EL = EC_1/EC_2 \times 100\%$ <sup>3,18</sup>.

#### **Superoxide dismutase activity, Catalase activity, Ascorbate peroxidase activity**

For SOD activity, cultures were crushed with acid washed sand and 2 mL of homogenization mixture prepared in potassium phosphate buffer (pH 7.8) containing 7 mM β-mercaptoethanol, 0.2% Triton-X 100 and 5 mM sodium ascorbate. The crushed cultures were centrifuged at 10000 ×g at 4°C for 10 min and 50 μL of the supernatant was mixed with

3 mL of reaction mixture containing 75 μM Nitroblue tetrazolium (NBT), 100 μM Ethylene diamine tetra acetic acid (EDTA) and 13 mM L-methionine. The initiation of the activity was started by adding 120 μL of 50 mM riboflavin. The reaction was carried in an aluminium foiled lined box containing 15 W fluorescent tube at the distance of 10 cm for 10 min. The absorbance of the reaction was taken at 560 nm. One unit of SOD activity was defined as the amount of enzyme causing 50% inhibition of photochemical reduction of NBT<sup>3,19</sup>.

For preparation of enzyme extract, the cultures were crushed with 50 mM phosphate buffer saline (PBS) pH7.0 and centrifuged at 12000 ×g at 4°C, for 10 min. 1.0 mL of the supernatant was further mixed with 1.5 mL of PBS and 10 μL of H<sub>2</sub>O<sub>2</sub>. The reaction was run for 2 min after adding the enzyme extract. The activity was recorded as per decrease in the initial linear rate of H<sub>2</sub>O<sub>2</sub> by taking absorbance at 240 nm<sup>20</sup>.

To determine APX activity in the cell, the homogenized cyanobacterial cultures, treated with different concentrations of iron, were crushed with acid washed sand in the presence of potassium phosphate buffer (20 mM, pH 7.0)<sup>21</sup>. The samples were centrifuged at 10000 ×g for 10 min at 4°C. 1.0 mL of potassium phosphate buffer (20 mM, pH 7.0), 1.0 mL of 4 mM ascorbic acid, 1 mL of 20 mM H<sub>2</sub>O<sub>2</sub> and finally 1.8 mL double distilled water was added to 200 μL of the supernatant. The reaction rate was observed as per decrease in absorbance at 290 nm compared with blank. The rate constant of reaction was calculated by using 2.8/mM/cm as extinction coefficient for ascorbate<sup>27</sup>.

#### **Proline, cysteine and non protein thiol estimation**

About 2 mL of well suspended cultures were centrifuged and the pellets were kept with 3 mL of 3% sulphosalicylic acid for 10 min acid and again centrifuged at 8000 ×g for 5 min. To the 1.0 mL supernatant, 1.0 mL of glacial acetic acid was added followed by addition of acidic ninhydrin solution prepared in 2:3 solutions of glacial acetic acid and 6 M orthophosphoric acid. The reaction was initiated by keeping it in water bath for 80°C for 1 h. The termination of reaction was done by keeping the test tube immediately in ice bath. 4 mL of toluene was added to the solution and the upper layer of toluene layer was taken for absorbance at 520 nm for the determination of proline<sup>3,23</sup>.

Two mL of well suspended culture was homogenized with perchloric acid and centrifuged at 8000 ×g for 10 min. To 1.0 mL supernatant, 1.0 mL

of glacial acetic acid was added followed by addition of 1.0 mL acidic ninhydrin solution prepared with the mixture of 6 mL of glacial acetic acid, 4 mL of HCl solution and 0.25 gm of ninhydrin. The solution was kept at 95°C (water bath) for 30 min and cooled down immediately. The absorbance was taken at 560 nm for determination of cysteine<sup>24</sup>.

To determine non protein thiol, 2 mL of well suspended culture was homogenized with treated with 2 mL of 3% sulphosalicylic acid and left for 10 min. The content was centrifuged at 8000 ×g for 10 min. To the supernatant (250 µL), 2.5 mL of reaction mixture was added which was prepared by Na-PO<sub>4</sub> buffer (pH 7.5) containing 100 mM EDTA and 100 mM DTNB (Ellman's reagent) [5' dithio-bis-(2 nitrobenzoic acid)]. The absorbance was taken at 412 nm<sup>25</sup>.

#### Statistical analysis

To describe the variation in the behaviour of the morphology and growth in *A. sphaerica* at different iron concentrations, Principal component analysis (PCA) was done using Biodiversity Pro version 2. The observed values were graphically represented using software Sigma Plot. 12. The level of significance of the morphological and physiological parameters were also analyzed with Pearson correlation using SPSS software (SPSS Inc. Version 16.0).

## Results and Discussion

### Selection of iron concentrations

Growth behaviour (in terms of direct absorbance and chlorophyll a content) was compared in *Anabaena sphaerica* at different concentrations of iron i.e. -FeCl<sub>3</sub> (0), 20, 50, 75, 100, 125, 150 µM FeCl<sub>3</sub> for 10 days (Fig. 1 A & B). It was found that *A. sphaerica* showed maximum absorbance and chlorophyll-a content at 20 µM followed by 50 µM and 75 µM FeCl<sub>3</sub>. Result also showed that *A. sphaerica* was poorly survived at 125 and 150 µM FeCl<sub>3</sub> concentrations, and hence these two concentrations were not taken for further experiments.

### Specific growth rate estimation

When *Anabaena sphaerica* was incubated at different concentrations of iron (FeCl<sub>3</sub>) i.e. 0, 20, 50, 75 and 100 µM FeCl<sub>3</sub>, it was observed that the cyanobacterium was remained in the exponential phase up to 6<sup>th</sup> day of incubation (Fig. 2A). FeCl<sub>3</sub> (20 µM) is the best suited concentration for the growth because iron may be sufficiently available at that time for proper functioning of all the iron requiring metabolic processes especially photosynthesis,

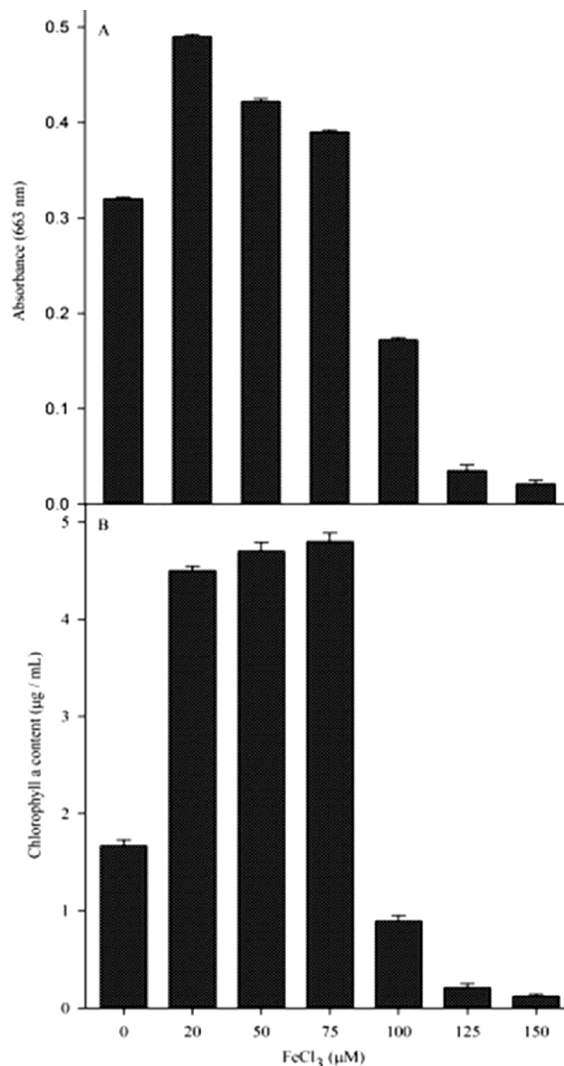


Fig. 1 — Growth behaviour in terms of (A) direct absorbance; and (B) chlorophyll content at different concentrations of iron in the cyanobacterium *Anabaena sphaerica* isolated from iron rich regions of Chhattisgarh. [Data represents the mean ± SD (n=6)]

nitrogen fixation and ultimately the growth rate. In contrast to this, 18.8 % of reduction in the growth at -Fe concentration may be due to poor availability of the iron. Possibly an iron storage protein, ferritin also be failed to fulfill the iron requirements for proper growth as compared to 20 µM FeCl<sub>3</sub> treated cells. Subsequently, reactive oxygen species were also generated at a greater extent in iron deficient condition that might be a reason for reduced growth of the cyanobacterium [Fig. 2A & 4C(i)]. Earlier, it has been reported that iron deficiency leads to the formation of an oxidative stress in *Anabaena* sp. PCC 7120<sup>3,4,26</sup>. Possibly, maximum reduction in growth (28 %) and structural deformities at 100 µM FeCl<sub>3</sub> were due to maximum ROS production [Fig. 2A,

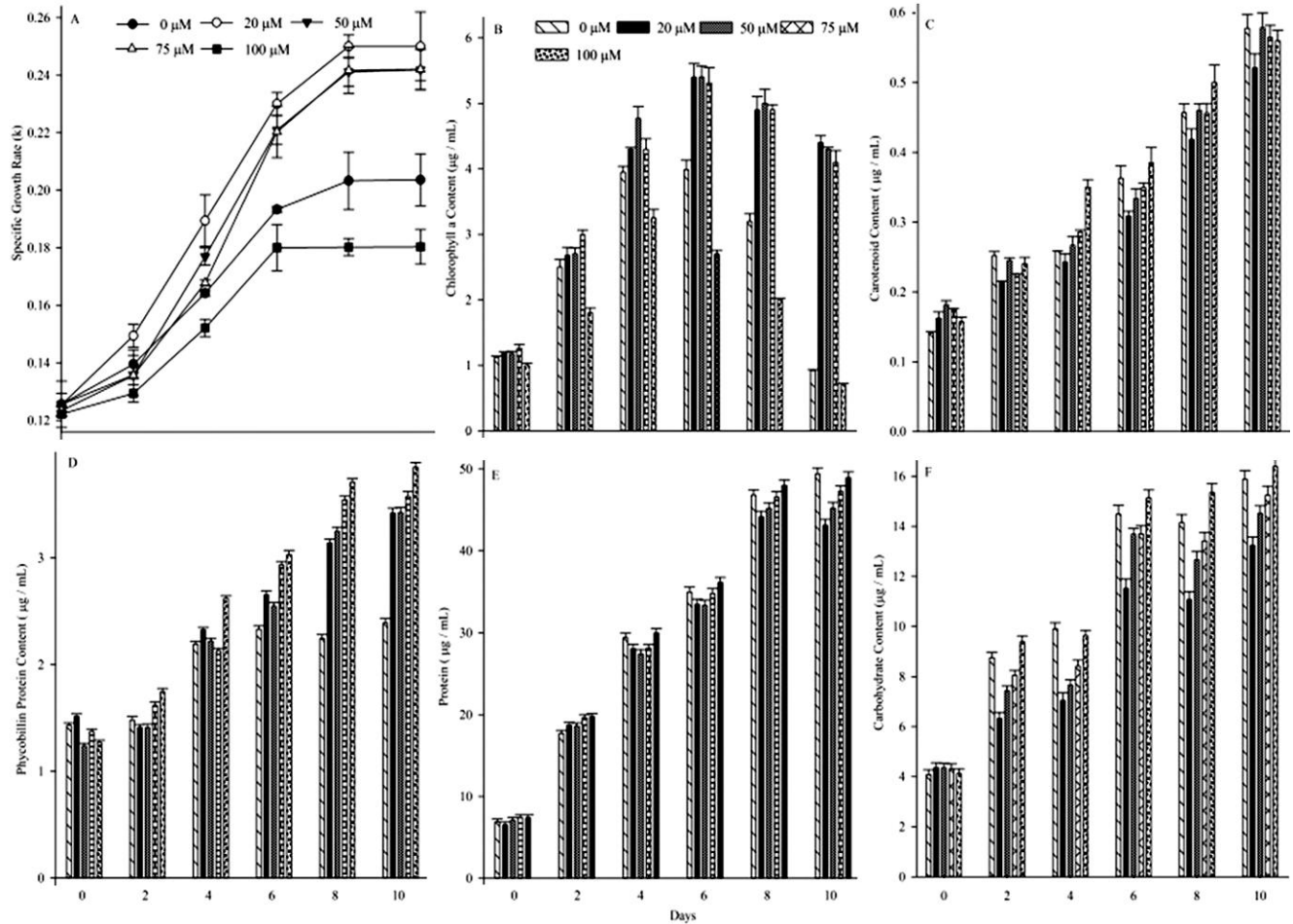


Fig. 2 — Growth pattern of *Anabaena sphaerica* in terms of (A) specific growth rate; (B) chlorophyll a content; (C) carotenoid content; (D) phycobillin protein; (E) protein; and (F) carbohydrate content at different concentrations of iron ( $\text{FeCl}_3$ ). [Data represents the mean  $\pm$ SD (n=6)]

4A(v), 4B(v) & 4C(v)]. Minimum reduction in growth at 50 and 75  $\mu\text{M}$   $\text{FeCl}_3$  concentrations was correlated with limited production of reactive oxygen species [Fig. 2A, 4C(iii) & 4C(iv)] and maximum involvement of available iron for the growth<sup>3</sup>.

#### Chlorophyll a, carotenoids and phycobillin content

It was evident from the result that as the culture aged, chlorophyll was continuously increased at all the tried concentrations i.e. 0, 20, 50 and 75  $\mu\text{M}$   $\text{FeCl}_3$ . But exception was seen in case of -Fe and 100  $\mu\text{M}$   $\text{FeCl}_3$  treated cells on the 10<sup>th</sup> day of incubation where the chlorophyll content was decreased by 79 and 84.1 % at the respective concentrations (Fig. 2B). The increment in phycobillin protein was observed from the 4<sup>th</sup> day of incubation (Fig. 2D). Maximum increment in the phycobillin was observed at 100 (3 times) followed by 75 (2.6 times), 50 (2.8 times) and 20  $\mu\text{M}$   $\text{FeCl}_3$  (2.2 times) from the initial

phycobillin content of the initial inocula. Growth in terms of phycobillin content was not so fast in absence of iron.

An increase in chlorophyll content and phycobillin protein at 50 and 75  $\text{FeCl}_3$  suggested that the surplus iron might have enhanced the biosynthesis of chlorophyll and phycobillin protein as reported in *Anabaena* sp. PCC7120<sup>4</sup>. The process of biosynthesis of chlorophyll and phycobillin protein depends on the level of chelated iron protoporphyrin<sup>27</sup>. An increase in the chlorophyll-a content and phycobillin protein during initial days (4<sup>th</sup> day of incubation) at iron deficient condition (-Fe) might be due to ferritin, which released iron for the synthesis of pigments. As the culture aged, continuous usage of iron from ferritin might be exhausted and caused decreased chlorophyll with constant phycobillin protein. It has been reported that the synthesis of protoporphyrin is

repressed due to an activation of iron responsive transcriptional regulator i.e. *Irr* under iron deprived condition. *irr* gene is expressed during iron limitation and initiates the formation of *Irr* protein that negatively regulates the  $\delta$ -amino levulinic acid dehydratase which is precursor of photosynthetic pigments chlorophyll and phycobillin protein<sup>27</sup>. Decrease in chlorophyll-a at iron deficient condition may also be due to replacement of ferredoxin by flavodoxin which is more expressed in such condition but have less catalytic capacity as that of ferredoxin<sup>28</sup>. Iron deficiency also results an improper electron oxidation of  $O_2^{\cdot-}$  and  $H_2O_2$  via electron reduction reaction that promotes schematic synthesis and accumulation of ROS within the chloroplast which are also one of the incentive for degradation of chlorophyll-a<sup>27</sup>. Decrease in chlorophyll content at higher concentration of iron (100  $\mu$ M) may be due to generation of ROS through Fenton's mechanism which was accumulated within chloroplast and led to chlorophyll degradation. Higher concentration of iron did not support photosynthetic activity in *Anabaena* sp. PCC 7120<sup>3</sup>. In our experimental organism *A. sphaerica*, phycobillin proteins were continuously increased during prolonged exposure of higher concentration (up to 10<sup>th</sup> day). Possibly, iron excessiveness resulted into the de-repression of *Irr* protein synthesis which promoted the production of protoporphyrin and the phycobillin protein (tetrapyrrole) synthesis as in *A. sphaerica*<sup>27</sup>.

As compared to the carotenoid content of the initial day, there was an increment (3-4 times) in the carotenoid content of *A. sphaerica* at all the tried concentrations of iron (Fig. 2C). The carotenoid content was always higher in 50 and 75  $\mu$ M  $FeCl_3$  than that of control (20  $\mu$ M) whereas highest content was reported from -Fe and 100  $\mu$ M  $FeCl_3$  treated cells. The elevated amount of carotenoid content in *A. sphaerica* in iron deprived condition and also in 100  $\mu$ M  $FeCl_3$  possibly for quenching increased level of ROS including  $H_2O_2$  (Fig. 2C, 4C(i), 4C(v) & 5C)<sup>20,29,30</sup>. It was evident from Fig. 4C(v) that ROS was generated maximally at higher concentration of  $FeCl_3$  in *Anabaena sphaerica*. Probably, increased carotenoid content blocked the oxygen activation and protected from photooxidation.

#### Protein and Carbohydrate content

Similar trend of increment in protein and carbohydrate content was followed at all the tried concentrations up to the last day of incubation

(Fig. 2 E & F). Maximum carbohydrate content was observed at -Fe (3.89 times) and 100  $\mu$ M (3.9 times) followed by 75 (3.53 times), 50 (3.3 times) and 20 (3.03 times)  $\mu$ M  $FeCl_3$  on the last day of incubation with respect to the carbohydrate content of the initial day (Fig. 2F).

The protein content was increased in *Anabaena sphaerica* under iron deficiency that might be correlated with the over expression of Isi A protein (CP43' protein) which is an effective energy quencher and protectant of the photosystems<sup>31</sup>. It is also well known that some specific types of small redox proteins like flavodoxin are expressed to replace iron containing ferredoxin. Therefore, the expression of flavodoxin may be one of the probable reasons for increased level of protein to maintain the growth of the cyanobacteria even at iron deficient condition at some extent<sup>32</sup>.

Elevated amount of protein content might also be correlated with the elevated amount of heat shock proteins and molecular chaperons which detoxified the over production of ROS at higher concentration of iron (100  $\mu$ M  $FeCl_3$ ). These HSPs binds with the cellular protein and maintains the structural folding of the protein and ultimately maintains the structural and functional integrity of the cell<sup>31,33</sup>. Apart from this, the level of ferritin protein might be also increased at 100  $\mu$ M  $FeCl_3$  to sequester excess iron within its cavity, and thus inhibits the iron induced generation of reactive oxygen species. Thus, ferritin protein also acts as protective agent for iron induced ROS detoxification<sup>34</sup>. Due to suboptimal level of ROS generation at 20, 50 & 75  $\mu$ M  $FeCl_3$ , additional proteins may not be required for the protection against the ROS.

Increment in the carbohydrate content of *Anabaena sphaerica* during iron deficiency can be correlated with the findings of Zocchi<sup>35</sup> where iron deficiency stimulated the carbohydrate concentration (glucose-6-phosphate) and decreased the concentration of starch. The catabolism of carbohydrate (starch) and activation of several glycolytic enzymes has been enhanced in iron deficient condition<sup>36</sup>. Secondly, carbohydrate may be increased due to gluconeogenesis during iron deficient condition<sup>35</sup>. Thirdly, elevated amount of ROS could have led to degradation of starch (polysaccharides) into the form of soluble sugar that may have played an important role in osmotic adjustment of *A. sphaerica* cells under iron deficient condition<sup>36</sup>.

**Heterocyst frequency, nitrogenase activity and morphological alterations**

Almost an equal heterocyst frequency at 20, 50 and 75  $\mu\text{M}$   $\text{FeCl}_3$  concentrations suggested the proper availability of iron at the 50 and 75  $\mu\text{M}$   $\text{FeCl}_3$  (as compared to 20  $\mu\text{M}$   $\text{FeCl}_3$ ) to perform normal

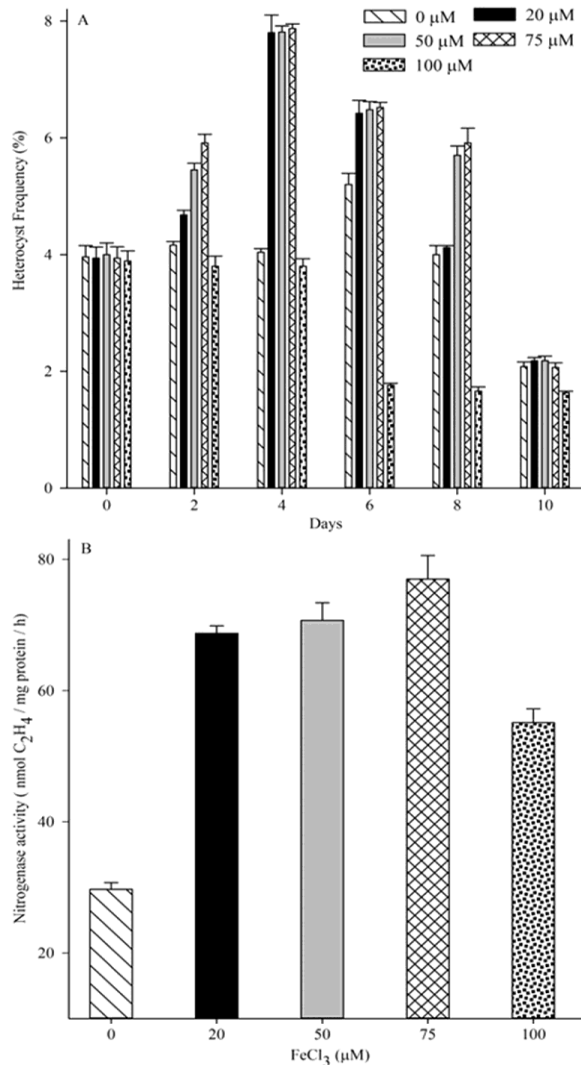


Fig. 3 — (A) Heterocyst frequency; and (B) Nitrogenase activity of *Anabaena sphaerica* at different concentrations of  $\text{FeCl}_3$ . [Data represents the mean  $\pm$  SD (n=6)]

cellular function i.e. nitrogen fixation occurs in the heterocyst (Fig. 3A & B). It is well known that the enzyme nitrogenase requires sufficient iron for its nitrogen fixation activity. So, absence of iron resulted decreased level of heterocyst frequency and nitrogenase activity in *Anabaena sphaerica* as observed in confocal photography [Fig. 4A(i)]. Confocal and SEM photography at highest iron concentration (100  $\mu\text{M}$ ) also proved the reduction in heterocyst frequency which might be due to the highest production of reactive oxygen species that ultimately altered the cellular structure (including heterocyst) of *A. sphaerica* (Fig. 4A(v), 4B(v), 4C(v) & Table 1). The structural organization was significantly affected by -Fe and 100  $\mu\text{M}$   $\text{FeCl}_3$  treated cells of *A. sphaerica*. The size of a vegetative cell and heterocyst was maximally reduced at 100  $\mu\text{M}$  followed by - $\text{FeCl}_3$  treated cell (Table 1). Confocal and SEM photographs clearly depicted a number of cellular deformities at the above concentrations [Fig. 4A(i), 4A(v), 4B(i) & 4B(v)]. One cell became spindle shaped in 100  $\mu\text{M}$   $\text{FeCl}_3$  treated cells. The cells were ruptured at higher concentration (100  $\mu\text{M}$   $\text{FeCl}_3$ ). The size of the vegetative cell and heterocyst were remained unchanged up to 75  $\mu\text{M}$   $\text{FeCl}_3$  but the spherical shape of the vegetative cell were transformed into sub spherical shape at 75  $\mu\text{M}$   $\text{FeCl}_3$  (Table 1). SEM photographs also showed more constrictions and septa within one cell at the same concentration. Cells were more elongated in 75 and 100  $\mu\text{M}$   $\text{FeCl}_3$ . Some cells were separated from one other.

**ROS, electrolyte leakage, MDA content and cellular H<sub>2</sub>O<sub>2</sub>**

The generated ROS in the cells of *A. sphaerica* at different concentrations of iron produces a green fluorescence after treated with DCFH-DA, a ROS sensing probe. Maximum green fluorescence were observed at 100  $\mu\text{M}$   $\text{FeCl}_3$  concentration proved the highest ROS production followed by -Fe, 75  $\mu\text{M}$  and 50  $\mu\text{M}$  [Fig. 4C(i), 4C(ii), 4C(iv) & 4C(v)]. Probably, the higher level of ROS generation in the cells of *A. sphaerica* was due to imbalances in electron

Table 1 — Representation of the shape and size of vegetative cell and heterocyst of *Anabaena sphaerica* treated with different concentrations of iron. [Data represents the mean  $\pm$  SD (n=6)]

Concentration ( $\text{FeCl}_3$ )	Initial Day				4 <sup>th</sup> Day			
	Veg. cell size ( $\mu\text{m}$ )	Shape	Heterocyst size ( $\mu\text{m}$ )	Shape	Veg. cell size ( $\mu\text{m}$ )	Shape	Heterocyst size ( $\mu\text{m}$ )	Shape
-Fe	2 $\pm$ 0.026	Spherical	2.5 $\pm$ 0.038	Sub-spherical	1.5 $\pm$ 0.007	Sub-spherical	2 $\pm$ 0.005	Sub-spherical
20 $\mu\text{M}$	2 $\pm$ 0.005	Spherical	2.5 $\pm$ 0.036	Sub-spherical	2 $\pm$ 0.005	Spherical	2.5 $\pm$ 0.038	Sub-spherical
50 $\mu\text{M}$	2 $\pm$ 0.050	Spherical	2.5 $\pm$ 0.034	Sub-spherical	2 $\pm$ 0.005	Spherical	2.5 $\pm$ 0.038	Sub-spherical
75 $\mu\text{M}$	2 $\pm$ 0.020	Spherical	2.5 $\pm$ 0.032	Sub-spherical	2 $\pm$ 0.005	Spherical	2.5 $\pm$ 0.038	Sub-spherical
100 $\mu\text{M}$	2 $\pm$ 0.050	Spherical	2.5 $\pm$ 0.038	Sub-spherical	1 $\pm$ 0.026	Sub-spherical	1.5 $\pm$ 0.070	Sub-spherical

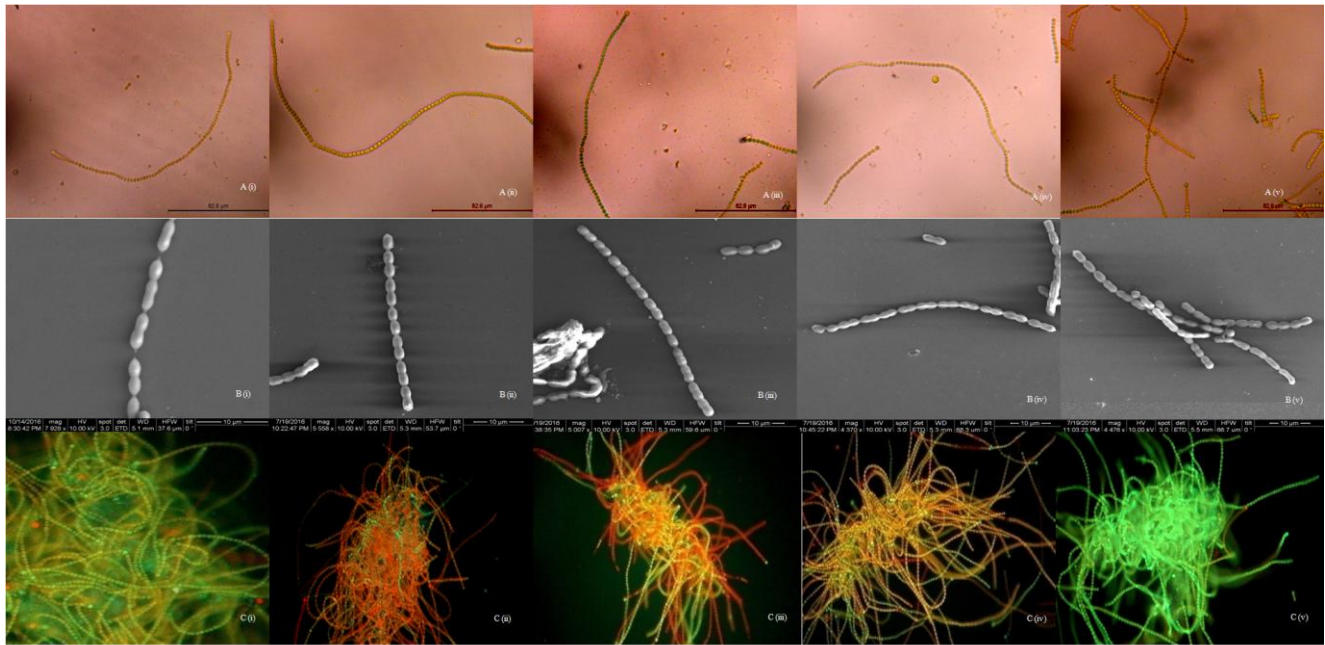


Fig. 4 — Images of A(i)-A(v) Confocal microscope; B(i)-B(v) SEM (10 μm); and C(i)-C(v) photographs of reactive oxygen species (ROS) generation of *Anabaena sphaerica* with respect to different concentrations (i-v) of iron ( $\text{FeCl}_3$ ) – 0, 20, 50, 75 & 100 μM, respectively

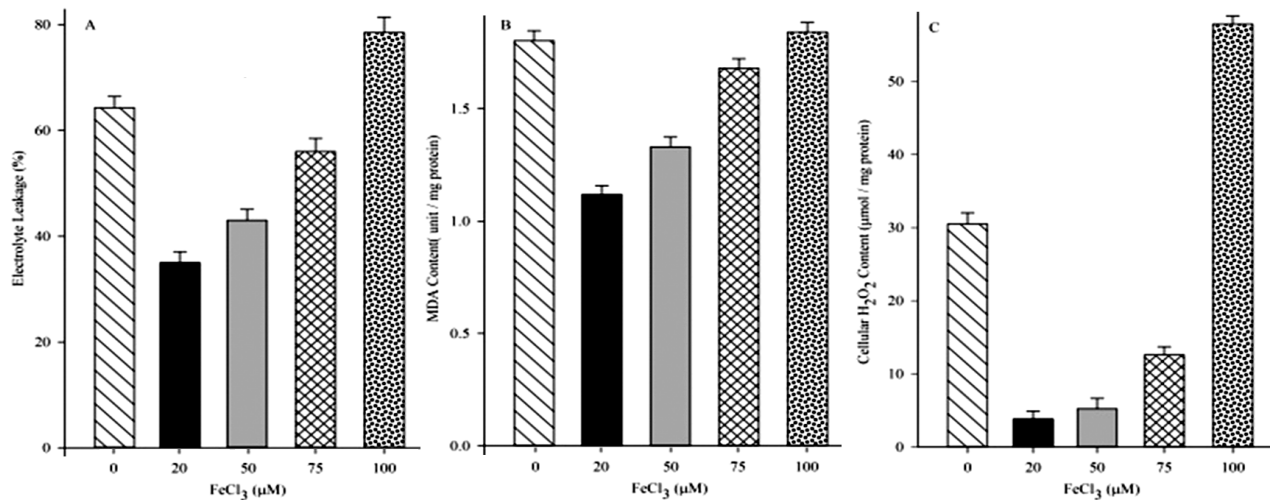


Fig. 5 — (A) Electrolyte leakage; (B) MDA content; and (C) Cellular  $\text{H}_2\text{O}_2$  of *Anabaena sphaerica* at different concentrations of  $\text{FeCl}_3$ . [Data represents the mean  $\pm$  SD (n=6)]

transport chain [Fig. 4C(i) & 4C(v)]. Further, membrane damage (in terms of electrolyte leakage) was maximally observed in 100 μM  $\text{FeCl}_3$  i.e. (78.5%) followed by -Fe (64.3 %). The other tried concentrations i.e. 20, 50 and 75 μM  $\text{FeCl}_3$  affected minimally and the integrity of cellular membrane was less damaged (35, 43 and 56%) (Fig. 5A).

In *Anabaena sphaerica*, highest Electrolyte leakage (EL) and MDA content were directly correlated with the highest ROS generation at -Fe and 100 μM  $\text{FeCl}_3$

[Fig. 4C(i), 4C(v), 5 A & B]. These generated ROS may peroxidize the membrane lipid especially the polyunsaturated fatty acids and ultimately disturbs the first line of defence structure i.e. membrane integrity. In contrary to this, highest lipid peroxidation and EL at higher iron concentration might be due to production of ROS i.e. hydroxyl radical via Fenton's mechanism<sup>39</sup>. It is well known that ROS binds with the methylene group of PUFA and results the formation of lipid alkoxyl radical and some aldehydes



(malondialdehydes, crotonaldehyde, acrolein), lipid epoxides and alcohol<sup>37</sup>. Minimum membrane damage was observed at 50 and 75  $\mu\text{M}$   $\text{FeCl}_3$  may be due to minimum ROS production which resulted into less peroxidation of lipid (MDA) and less leakage of ions<sup>14,32</sup>.

As the concentration of iron increased, cellular  $\text{H}_2\text{O}_2$  was also increased in *Anabaena sphaerica* and it was maximum at 100  $\mu\text{M}$  (15.13 times) followed by 75  $\mu\text{M}$  (3.29 times) and 50  $\mu\text{M}$   $\text{FeCl}_3$  (1.36 times), respectively than that of 20  $\mu\text{M}$   $\text{FeCl}_3$  (Fig. 5C). Increased production of  $\text{H}_2\text{O}_2$  at higher concentrations of iron might be due to spare iron molecules which sequentially synthesized ROS ( $\text{O}_2^{\cdot-}$ ,  $\text{H}_2\text{O}_2$ ,  $\text{OH}^{\cdot}$ ) through Haber-Weiss and Fenton's mechanism<sup>37</sup>.

#### Antioxidative enzymatic activity

The super oxide dismutase activity (SOD) was increased in proportion to  $\text{FeCl}_3$  concentrations in the medium (Fig. 6A). Under  $-\text{FeCl}_3$  condition, SOD activity was lowest even though cell produced a considerable amount of  $\text{H}_2\text{O}_2$ . It means iron unavailability has caused oxidative stress as suggested by Kaushik *et al.*<sup>20</sup>. Possibly, the absence of iron formed  $\text{H}_2\text{O}_2$  due to activation of some other ROS generating systems i.e. NADH/NADPH oxidase in plasma membrane or cell wall,  $\beta$ -oxidation of fatty acid, xanthin oxidase in peroxisomes, amine oxidase in apoplast as reported by Singh *et al.*<sup>26</sup>. Minimum production of SOD activity at  $-\text{FeCl}_3$  condition suggested the importance of iron in synthesis of SOD enzyme. Since antioxidative enzyme superoxide dismutase sustains in four isozymes MnSOD, FeSOD, CuSOD and ZnSOD which require these trace

element as a cofactor depending on their location (Fig. 6A). Absence of iron may restrict the activity of SOD (probably FeSOD). Result also suggested that increased  $\text{H}_2\text{O}_2$  in accordance with concentration (20-100  $\mu\text{M}$   $\text{FeCl}_3$ ) may be correlated to the proportionate increase in SOD activity that converted ROS ( $\text{O}_2^{\cdot-}$ ) into less toxic  $\text{H}_2\text{O}_2$  as reported in Singh *et al.*<sup>26</sup>. Similar findings have also been reported in the algal and cyanobacterial cells<sup>38-40</sup>.

When the Catalase (CAT) activity of *Anabaena sphaerica* was examined at different concentrations of iron, it was observed that there was a gradual increase in CAT activity from  $-\text{FeCl}_3$  concentration to 75  $\mu\text{M}$  concentration of iron. But at 100  $\mu\text{M}$  concentration, CAT activity was highly reduced which was almost 54% activity of controlled value (Fig. 6B). The maximum ascorbate peroxidase activity (APX) was investigated in 100  $\mu\text{M}$  treated cells followed by iron deficient condition (Fig. 6C).

It has been proved that catalase activity was lowest in 100  $\mu\text{M}$   $\text{FeCl}_3$  followed by  $-\text{Fe}$  whereas APX activity was highest in 100  $\mu\text{M}$   $\text{FeCl}_3$  followed by  $-\text{Fe}$  condition (Fig. 6 B & C). Decrease CAT activity in iron deficient condition might be due to less availability of iron which is an integral part of the catalase enzyme<sup>39</sup>. Secondly, catalase has the lower affinity towards  $\text{H}_2\text{O}_2$  compared to APX. Probably, maximum  $\text{H}_2\text{O}_2$  produced by superoxide dismutase under iron deficient condition was detoxified by APX and resulted the decreased catalase activity in *A. sphaerica* as reported in *Anabaena sp.* PCC7120<sup>3,37</sup>. As the concentration of iron was increased, SOD and APX activity was also increased up to 100  $\mu\text{M}$   $\text{FeCl}_3$

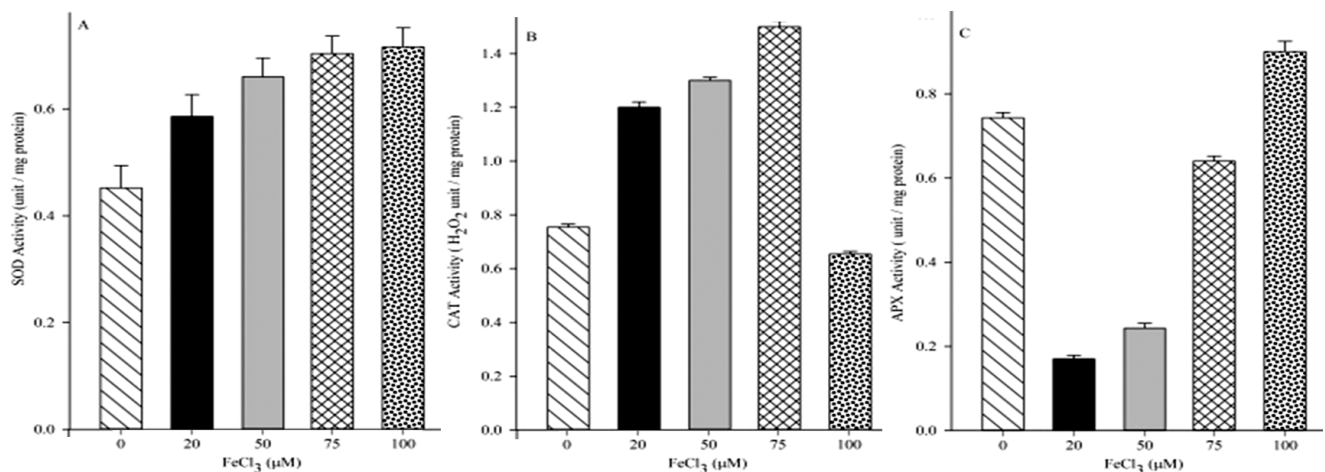


Fig. 6 —Changes in (A) superoxide dismutase (SOD); (B) catalase (CAT); and (C) Ascorbate peroxidase (APX) activity of *Anabaena sphaerica* at different concentrations of  $\text{FeCl}_3$ . [Data represents the mean  $\pm$  SD (n=6)]

(compared to 20  $\mu\text{M}$ ) but the catalase activity was increased only up to 75  $\mu\text{M}$   $\text{FeCl}_3$ . It indicates that catalase activity worked more efficiently up to 75  $\mu\text{M}$   $\text{FeCl}_3$  and maximum  $\text{H}_2\text{O}_2$  was degraded by catalase and APX up to 75  $\mu\text{M}$   $\text{FeCl}_3$ . But as the concentration increased (100  $\mu\text{M}$   $\text{FeCl}_3$ ), maximum generated  $\text{H}_2\text{O}_2$  would have been degraded most efficiently by APX as reported in other cyanobacteria (Figs. 5C & 6C)<sup>38</sup>. It is well known that Ascorbate peroxidase activity showed higher affinity towards  $\text{H}_2\text{O}_2$ <sup>37</sup>. Possibly, Fur (ferric uptake regulator) bound with  $\text{Fe}^{2+}$  and acted as a repressor for iron responsive genes including catalase enzyme at 100  $\mu\text{M}$   $\text{FeCl}_3$  in *A. sphaerica*. Similar reports were also observed in *Anabaena* sp. where over expression of Fur A resulted into four-fold reduction in CAT activity<sup>41</sup>.

#### Non enzymatic antioxidant activity

In our experimental findings, increased proline under iron deficient condition (Fig. 7A) was directly related to the elevated amount of ROS as reported in *Anabaena* sp. PCC 7120<sup>2</sup> because proline can easily quench ROS. Maximum proline content at iron 100  $\mu\text{M}$   $\text{FeCl}_3$  might chelate the excess iron and reduced their toxic effect in *A. sphaerica* as was observed in *Armeria maritima* where elevated proline forms copper-proline complex<sup>42</sup>. It may be assumed that higher iron concentration (100  $\mu\text{M}$   $\text{FeCl}_3$ ) have enhanced proline biosynthesis enzymes  $\Delta$ pyrroline-5-carboxylate reductase or ornithine  $\delta$ -amino transferase as reported in response to various abiotic stresses<sup>42</sup>. Proline is also known as chemical chaperon that is capable to scavenge ROS by enhancing and stabilizing antioxidative enzymes (catalase, superoxide dismutase and peroxidase) and proteins<sup>41</sup>. Moreover, the essential role of proline in metal tolerance has also recently been shown in cyanobacterial cells<sup>43</sup>.

As the  $\text{FeCl}_3$  was supplemented in iron deficient medium, cysteine was going on increased and maximum was observed at 100  $\mu\text{M}$   $\text{FeCl}_3$  treated cells (Fig. 7B). An increase in the cysteine content of *A. sphaerica* at the elevated concentrations of iron was accordance with the findings where cysteine was increased against  $\text{Hg}^{39}$ . A continuous elevation in iron concentration might increase the sulphate reduction pathway that ultimately induced the synthesis of ATP sulfurylase and adenosine 5'-phosphosulfate sulphotransferase to fulfill the requirement of phytochelatin synthesis. Phytochelatin synthesis. Phytochelatin are basically cysteine enriched compounds, where cysteine exists as a free residue of sulphahydril group and acts as a

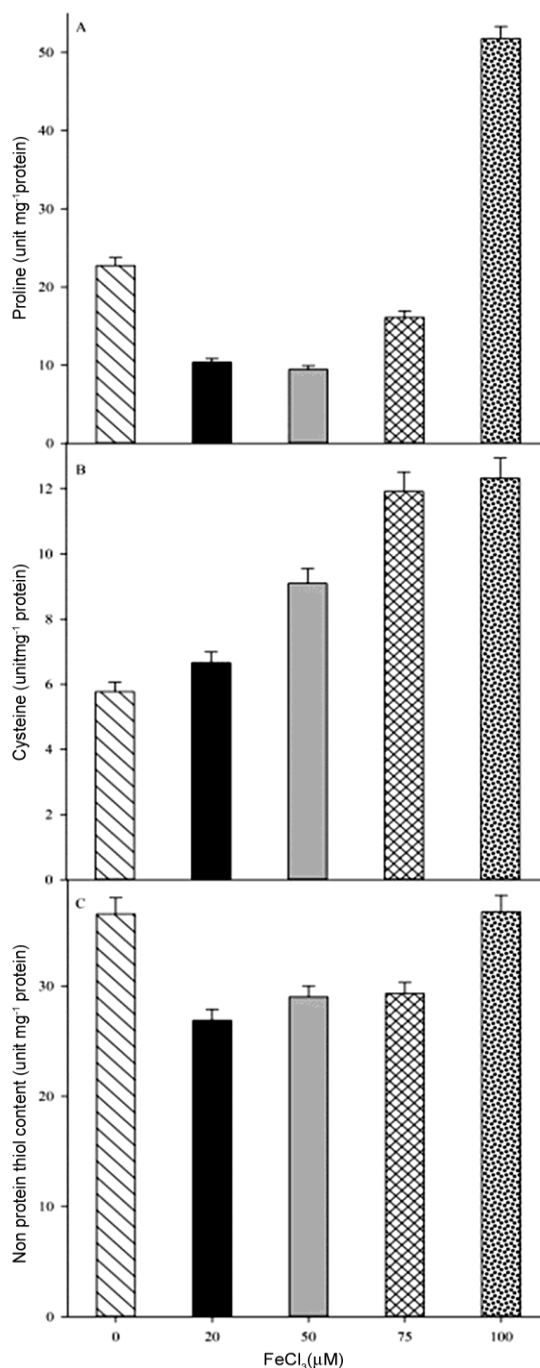


Fig. 7 — (A) Proline content; (B) cysteine; and (C) non protein thiol content of *Anabaena sphaerica* at different concentrations of  $\text{FeCl}_3$ . [Data represents the mean  $\pm$  SD (n=6)]

metal chaperon. Recently, phytochelatin production has been reported to mitigate oxidative stress in *Anabaena doliolum*<sup>42</sup>.

Cysteine is actually the key component of tripeptide ( $\gamma$ -glutamyl-cysteine-glycine) glutathione an important non protein thiol. Thiol groups have an

Table 2 — Correlation coefficient of (r) at the P value 0.01 levels obtained via Pearson method for the morphological and physiological activities of *Anabaena sphaerica* treated with different concentrations of iron

Days	Vegetative cell size	Heterocyst size	Heterocyst frequency	Specific growth rate	Chl a content	Carotenoid content	Phycobillin content	Protein content	Carbohydrate content	
-FeCl <sub>3</sub>	1.00*	-0.520*	-0.858*	0.934*	-0.460	0.430	0.979*	0.877*	0.985*	0.950*
20 μM	1.00*	-0.163	-0.373	0.963*	-0.319	0.792*	0.972*	0.983*	0.968*	0.963*
50 μM	1.00*	-0.062	0.187	0.960*	-0.263	0.757*	0.970*	0.983*	0.980*	0.936*
75 μM	1.00*	-0.042	-0.682*	0.963*	0.279	0.754*	0.831*	0.939*	0.980*	0.960*
100 μM	1.00*	-0.819*	0.515*	0.931*	-0.894*	-0.052	0.991*	0.983*	0.709*	0.943*

[Correlation is significant at the 0.01 level (2-tailed)]

ability to scavenge ROS and the products of lipid oxidation<sup>44</sup>. Our results also proved that maximum production of thiol was only to detoxify the maximum ROS and MDA content generated in -Fe and 100 μM FeCl<sub>3</sub> treated cells (Fig. 4C(i), 4C(v), 5B & 7C).

Almost equal amount of non protein thiol content was observed at 50 and 75 μM FeCl<sub>3</sub> which was slightly enhanced in comparison to control (1.08 to 1.09 times of control) (Fig. 7C). Increased level of thiol at -Fe and FeCl<sub>3</sub> (100 μM) might be contributed its protective role in association of cysteine in maintaining the rigidity of the proteins<sup>32</sup>. Increased cysteine and thiol content were also reported against other stresses such as low light exposure, higher concentration of mercury and UV-B exposure<sup>30,39,45</sup>.

#### Statistical analysis

The correlation was tested among iron concentrations and their impact on the morphological and physiological behaviour of *A. sphaerica*. The vegetative cell size and heterocyst size was found to be negatively and significantly correlated to -FeCl<sub>3</sub> ( $r = -0.520$ ,  $-0.858$ ) and 100 μM FeCl<sub>3</sub> ( $r = -0.819$ ,  $-0.515$ ) concentration. The specific growth rate was found to be negatively correlated with 100 μM FeCl<sub>3</sub> iron concentration ( $r = -0.931$ ). The chlorophyll-a content was found to be positively correlated with 20, 50 and 75 μM iron concentrations. However, the carotenoid, phycobillin protein, protein and carbohydrate was found to be positively and significantly correlated with all the tried iron concentrations (Table 2).

As evident from the scattered plot generated through a software Bio Diversity Pro version 2 using the obtained data (Fig. 8), revealed that the size of vegetative cell and heterocyst, heterocyst frequency, specific growth rate and chlorophyll-a content were negatively correlated with PC 1 at 100 μM FeCl<sub>3</sub> whereas only carotenoid content, protein and carbohydrate were negatively affected with PC 1 at

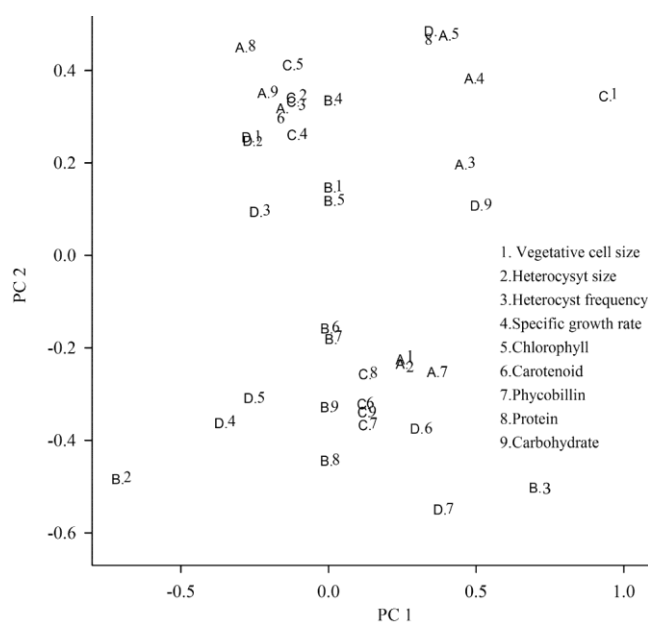


Fig. 8 — Representation of principal component analysis (PCA) showing effect of different concentrations of iron (FeCl<sub>3</sub>) on the morphological and growth parameters of cyanobacterium *A. sphaerica*

-FeCl<sub>3</sub> condition. Phycobillin protein was positively correlated with PC 1 at -FeCl<sub>3</sub> and 100 μM FeCl<sub>3</sub>. The photosynthetic pigments were significantly negatively correlated with PC 2 at 100 μM FeCl<sub>3</sub> whereas the size of vegetative cell and heterocyst were found to be negatively correlated with PC 2 at -FeCl<sub>3</sub> condition. Presence (100 μM FeCl<sub>3</sub>) and the absence of iron made positive correlation between the parameters i.e. specific growth rate, protein, carbohydrate, heterocyst frequency, chlorophyll-a and PC 2.

Overall, a possible mechanism of toxicity and defence strategies adopted by the cyanobacterium *A. sphaerica* against iron deprived and iron sufficient conditions has been summarized in Fig. 9.

Thus, it can be concluded that almost same level of structural and physiological alterations were observed

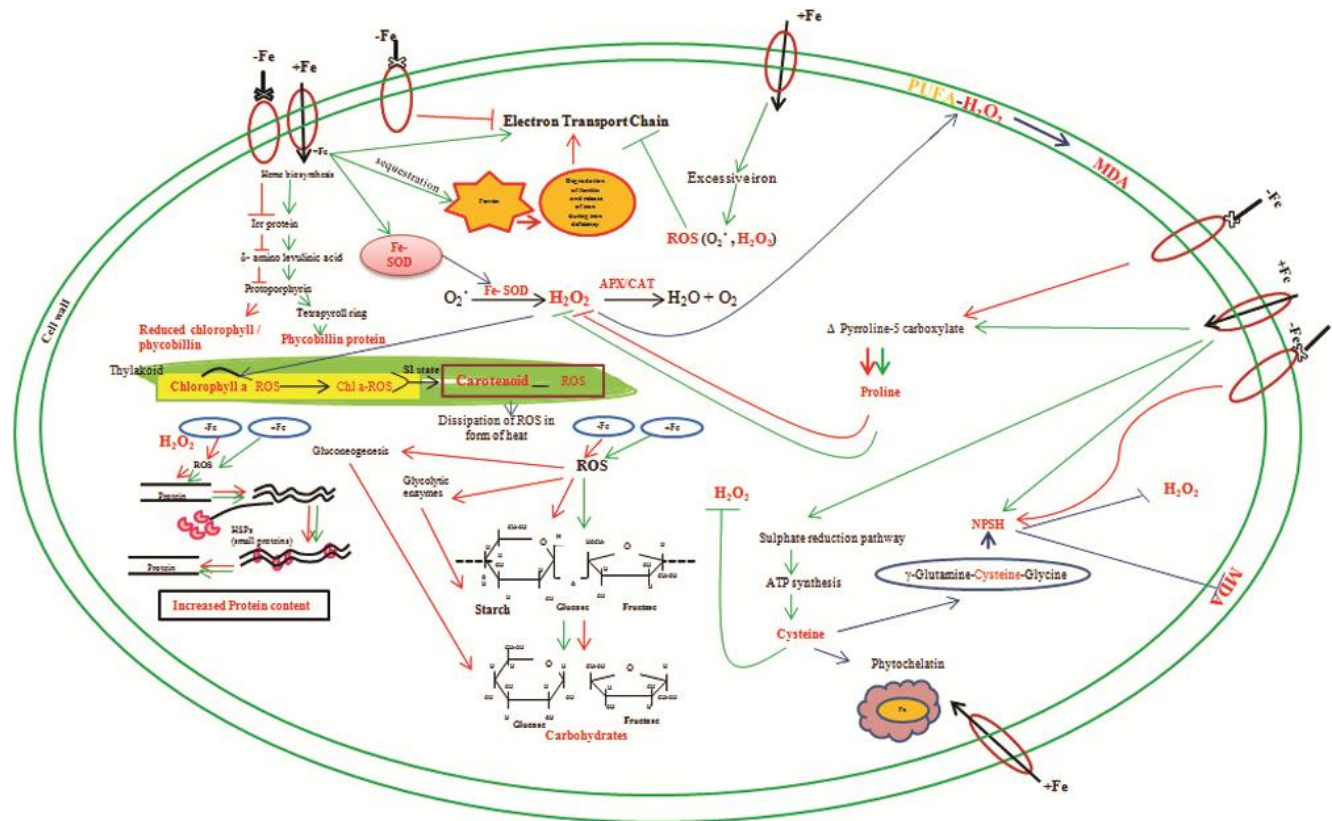


Fig. 9 — Schematic representation of toxicity (ROS production) and defence strategies against iron deprived and iron sufficient conditions in cyanobacterium *Anabaena sphaerica*, isolated from iron rich region of Chhattisgarh, India. Red written matters denote parameters evaluated in *A. sphaerica*; Red arrow denotes pathway of iron deprived condition; Green arrow denotes pathway for presence of iron and blue arrow denotes pathway for both absence and presence of iron

in *A. sphaerica* at higher dose of iron (100  $\mu\text{M}$   $\text{FeCl}_3$ ) and in iron deficient condition (-Fe) but both the conditions used different preventive measures for survival. Antioxidative enzyme activities i.e. SOD and APX along with antioxidants (proline, cysteine, carotenoid and non-protein thiol) are more evolved at 100  $\mu\text{M}$   $\text{FeCl}_3$  whereas in case of -Fe condition, APX activity and proline and non protein thiol content are more strengthened to protect the cyanobacterial against iron tolerance. At 50 and 75  $\mu\text{M}$   $\text{FeCl}_3$ , structural and functional integrity is almost unaltered and may be correlated with minimum induced toxicity and maximum tolerance due to an efficient ROS detoxification processes which pave a way to grow such cyanobacterium *Anabaena sphaerica* in iron rich paddy soils.

### Acknowledgement

We are thankful to funding agency UGC and CSIR, New Delhi for providing financial support.

### Conflict of interest

Authors declare no conflict of interests.

### References

- 1 Kaushik MS & Mishra AK, Iron induced modifications in physiological attributes and SDS-PAGE of whole cell proteins patterns of *Anabaena* PCC7120 and its derivatives *ntcA* mutant. *Indian J Biotechnol*, 14 (2015) 93.
- 2 Singh A, Mishra AK, Singh SS, Sarma HK & Shukla E, Influence of iron and chelator on siderophore production in *Frankia* strains nodulating *Hippophae salicifolia* D Don. *J Basic Microbiol*, 48 (2008) 111.
- 3 Kaushik MS, Srivastava M, Verma E & Mishra AK, Role of manganese in protection against oxidative stress under iron starvation in cyanobacterium *Anabaena* 7120. *J Basic Microbiol*, 54 (2014) 12.
- 4 Saxena RK, Raghuvanshi R, Singh S & Bisen P, Iron induced metabolic changes in diazotrophic cyanobacterium *Anabaena* PCC 7120. *Indian J Exp Biol*, 44 (2006) 851.
- 5 Rippka R, Deruelles J, Waterbury JB, Herdman M & Stanier RY, Generic assignments, strain histories and properties of pure cultures of cyanobacterial. *J Gen Microbiol*, 111 (1979) 61.

- 6 Komárek J & Anagnostidis K, Modern approach to the classification system of cyanophytes 4 Nostocales. *Arch für Hydrobiol Supplemt*, 82 (1989) 345.
- 7 Singh SS, Singh P, Kunui K & Minj RA, Diversity analysis and distribution pattern of cyanobacteria isolated from different sites of Chhattisgarh, India. *J Asia Pacific Biodivers*, 7 (2014) 470.
- 8 Kratz WA & Myers J, Nutrition and growth of several blue green algae. *Am J Bot*, 42(1955) 287.
- 9 Mackinney G, Absorption of light by chlorophyll solutions. *J Biol Chem*, 140 (1941) 322.
- 10 Sarada R, Pillai MG & Ravishankar GA, Phycocyanin from *Spirulina* sp. influence of processing of biomass on phycocyanin yield, analysis of efficacy of extraction methods and stability studies on phycocyanin. *Process Biochem*, 34 (1999) 801.
- 11 Lowry OH, Rosebrough NJ, Farr AL & Randall RJ, Protein measurement with the Folin phenol reagent. *J Biol Chem*, 193 (1951) 75.
- 12 Bennett A & Bogorad L, Complementary chromatic adaptation in filamentous Blue Green alga. *J Cell Biol*, 58 (1973) 435.
- 13 DuBois M, Gilles KA, Hamilton JK, Roberts PA & Smith F, Colorimetric method for determination of sugars and related substances. *Analytical Chem*, 28 (1956) 356.
- 14 Singh SS, Upadhyay RS & Mishra AK, Physiological interactions in *Azolla-Anabaena* system adapting to the salt stress. *J Plant Interact*, 3 (2008) 155.
- 15 Mishra AK & Singh SS, Protection against salt toxicity in *Azolla pinnata-Anabaena azollae* symbiotic association by using combined-N sources. *Acta Biol Hung*, 57 (2006) 355.
- 16 Lee MY & Shin HW, Cadmium-induced changes in antioxidant enzymes from the marine alga *Nannochloropsis oculata*. *J Appl Phycol*, 15 (2003) 19.
- 17 Heath RI & Packer I, Photoperoxidation in isolated chloroplasts: 1. Kinetic and stoichiometry of fatty acid peroxidation. *Arch Biochem Biophys*, 125 (1968) 198.
- 18 Dionisio-Sese MI & Tobita S, Antioxidant response of rice seedlings to salinity stress. *Plant Sci*, 135 (1998) 9.
- 19 Stewart RRC & Bewley JD, Lipid peroxidation associated with accelerated ageing of soyabean axes. *Plant Physiol*, 65 (1980) 258.
- 20 Kaushik MS, Srivastava M, Srivastava A, Singh A & Mishra AK, Nitric oxide ameliorates the damaging effects of oxidative stress induced by iron deficiency in cyanobacterium *Anabaena* 7120. *Environ Sci Pollut Res*, 23 (2016) 21805.
- 21 Nakano Y & Asada K, Hydrogen peroxide is scavenged by ascorbate-specific peroxidase in spinach chloroplasts. *Plant Cell Physiol*, 22 (1981) 880.
- 22 Aono M, Sagi H, Fujiyama K, Sugita M, Kondo N & Tanaka K, Decrease in the activity of glutathione reductase enhances paraquat sensitivity in transgenic *Nicotiana tabacum*. *Plant Physiol*, 107 (1995) 48.
- 23 Bates LS, Waldren RP & Teare ID, Rapid determination of free proline for water stress studies. *Plant Soil*, 39 (1973) 207.
- 24 Gaitonde MK, A spectrophotometric method for the direct determination of cysteine in the presence of other naturally occurring amino acids. *Biochem J*, 104 (1967) 633.
- 25 Ellmann GL, Tissue sulfhydryl groups. *Arch Biochem and Biophys*, 82 (1959) 77.
- 26 Singh S, Pandey B, Agrawal SB & Agrawal M, Modification in spinach response to UV-B radiation by nutrient Management: Pigments, antioxidants and metabolites. *Indian J Exp Biol*, 56 (2018) 922.
- 27 Busch AWU & Montgomery B, Interdependence of tetrapyrrole metabolism, the generation of oxidative stress and the mitigative oxidative stress response. *Redox Biol*, 4 (2015) 260.
- 28 Tognetti VB, Zurbriggen MD, Morandi EN, Fillat MF, Valle EM, Hajirezaei MR & Carrillo N, Enhanced plant tolerance to iron starvation by functional substitution of chloroplast ferredoxin with a bacterial flavodoxin. *Proc Natl Acad Sci USA*, 104 (2007) 11500.
- 29 Kumar J, Parihar P, Singh R, Singh VP & Prasad SP, UV-B induces biomass production and nonenzymatic antioxidant compounds in three cyanobacterial. *J Appl Phycol*, 28 (2016) 140.
- 30 Rajan I, Rabindran R, Jayasree PR & Kumar PRM, Antioxidant potential and oxidative DNA damage preventive activity of unexplored endemic species of *Curcuma*. *Indian J Exp Biol*, 52 (2014) 138.
- 31 Ivanov AG, Krol M, Sveshnikov D, Selstam E, Sandström S, Koochek M, Park Y, Vasil'ev S, Bruce D, Öquist G & Huner NPA, Iron deficiency in cyanobacteria causes monomerization of photosystem I trimers and reduces the capacity for state transitions and the effective absorption cross section of photosystem I *in vivo*. *Plant Physiol*, 141 (2006) 1445.
- 32 Merlos MA, Michálek P, Kryštofová O, Zítka O, Adam V & Kizek R, The role of phytochelatins in plant and animals: A review. *J Metallom Nanotechnol*, 4 (2014) 27.
- 33 Srivastava A, Singh A, Singh SS & Mishra AK, Salt stress-induced changes in antioxidative defense system and proteome profiles of salt-tolerant and sensitive *Frankia* strains. *J Environ Sci Health A*, 52 (2017) 420.
- 34 Srivastava A & Mishra AK, Regulation of nitrogen metabolism in salt tolerant and salt sensitive *Frankia* strains. *Indian J Exp Biol*, 52 (2014) 358.
- 35 Zocchi G, Metabolic changes in iron stressed dicotyledonous plants. In: *Iron nutrition in plant and rhizospheric microorganism*, (Eds. Barton LL & Abadia J; Springer, Netherland), 2006, 369.
- 36 Hell R & Stephan UW, Iron uptake, trafficking and homeostasis in plants. *Planta*, 216 (2003) 551.
- 37 Sharma P, Jha AB, Dubey RS & Pessarakali M, Reactive oxygen species, oxidative damage, and antioxidative defense mechanism in plants under stressful conditions. *J Bot*, 2012 (2012) 26.
- 38 Singh R, Srivastava PK, Singh VP, Dubey G & Prasad SM, Light intensity determines the extent of mercury toxicity in the cyanobacterium *Nostoc muscorum*. *Acta Physiol Plantarum*, 34 (2012) 1131.
- 39 Mallick N & Mohn FH, Reactive oxygen species: response of algal cells. *J Plant Physiol*, 157 (2000) 193.
- 40 Chakraborty S, Mishra A, Verma E, Tiwari B, Mishra AK & Singh SS, Physiological mechanisms of

- aluminum (Al) toxicity tolerance in nitrogen-fixing aquatic macrophyte *Azolla microphylla* Kaulf: phytoremediation, metabolic rearrangements, and antioxidative enzyme responses. *Environ Sci Pollut Res*, 26 (2019) 9041.
- 41 González A, Bes MT, Barja F, Peleato ML & Fillat MF, Overexpression of Fur A in *Anabaena* sp. PCC 7120 reveals new targets for this regulator involved in photosynthesis, iron uptake and cellular morphology. *Plant Cell Physiol*, 51 (2010) 1914.
- 42 Liang X, Zhang L, Natarajan SK & Becker DF, Proline mechanisms of stress survival. *Antioxidants and Redox Signalling*, 19 (2013) 1011.
- 43 Chakraborty S & Mishra AK, Mitigation of zinc toxicity through differential strategies in two species of the cyanobacterium *Anabaena* isolated from zinc polluted paddy field. *Environ Pollut*, 263 (2020) 114375.
- 44 Bhargava P, Srivastava AK, Urmil S & Rai LC, Phytochelatin plays a role in UV-B tolerance in N<sub>2</sub> fixing cyanobacterium *Anabaena doliolum*. *J Plant Physiol*, 162 (2005) 1225.
- 45 Gayathri Murukesan G, Lynch F, Allahverdiyeva Y & Kosourov S, Acclimation responses of immobilized N<sub>2</sub>-fixing heterocystous cyanobacteria to long-term H<sub>2</sub> photo-production conditions: carbon allocation, oxidative stress and carotenoid production. *J App Phycol*, 31 (2019) 131.